Mechanics Research Communications 67 (2015) 34–38

Contents lists available at ScienceDirect

Mechanics Research Communications

journal homepage: www.elsevier.com/locate/mechrescom

A 1D model for the dynamic analysis of magneto-electro-elastic beams with curved configuration

M.T. Piovan[a,b,*], J.F. Olmedo Salazar[b]

[a] Centro de Investigaciones de Mecánica Teórica y Aplicada, Universidad Tecnológica Nacional FRBB, 11 de Abril 461, B8000LMI Bahía Blanca, Argentina
[b] Universidad de las Fuerzas Armadas-ESPE, Departamento de Ciencias de la Energía y Mecánica, Avda Rumiñahui S/N, Sangolqui, Pichincha, Ecuador

ARTICLE INFO

Article history:
Received 17 January 2015
Received in revised form 19 April 2015
Accepted 12 May 2015
Available online 21 May 2015

Keywords:
Curved beams
MEE
Dynamics
Flexible structures

ABSTRACT

The scope of the present paper is to present some new contributions in the dynamics of curved/straight MEE beams. The structure consists of a curved beam constructed with ceramic/metallic materials whose elastic behavior can be modified by influence of electro-magnetic fields. The problem of coupled elastic, electric and magnetic fields is briefly explained and the motion equations for curved members are introduced. An equivalent model for a MEE curved beam is then deduced appealing to a few constitutive hypotheses that enable the derivation of the electric–magnetic fields acting on the beam in preferential and prescribed directions. The theoretical topics covered in the model include shear flexibility due to bending as well as coupled elastic-electro-magnetic terms, among others. The model can be reduced to other models (straight beams or curved beams) by dropping terms or the magneto-electric fields and/or geometric parameters. Comparisons with the available models (for the reduced case of straight beam) and 2D models evaluated in the context of finite element methodologies are presented as well.

1. Introduction

Special composite materials consisting of piezoelectric and piezomagnetic components are used in smart structures. These type of intelligent structures have a coupled magneto-electro-elastic behavior that can be useful in many engineering devices. The recent high technology developments, specially in sensors, actuators, hydrophones, etc., that use smart materials, have stimulated the study and analysis of the coupled elastic, electric and magnetic behavior of structures constructed with such smart materials. The smart structures provide remarkable capabilities of sensing and reacting to external actions and/or disturbances, also satisfying reliability, light weight and the appropriate performances demanded in high-tech structural applications [1–3].

During the last 10 year many researchers have been devoting their attention to the development of technical models for studying the mechanical response (statics, dynamics, instability, etc) of the so-called magneto electro elastic (MEE) structures. An interesting variety of models of MEE structures has been introduced principally for piezoelectric and piezomagnetic plates and shells [4–7]. In these articles the 3D static behavior of multilayered MEE strips and plates were analyzed. These structures were subjected to sinusoidally distributed magnetic, electric and mechanic loads. Dynamic counterparts of the aforementioned works have been performed by Chen et al. [8], Pan and Heyliger [9] among others. Moreover Wu and Lu [10] and Tsai et al. [11] among others studied the dynamics responses of shells and plates appealing to 3D formulations.

All aforementioned research articles were focused in rectangular plates and shells or at least shells with slight geometrical complications, i.e. for example simply or doubly curved profile. According to a thorough bibliographical review, it is important to remark that there are quite few articles related to the study of MEE slender structures in the context of a beam model or theory. The papers of Milazzo and coworkers [12–14] are the very firsts where studies about the dynamics of MEE beams (in the context of extended Bernoulli–Euler and/or Timoshenko theories) have been carried out, and besides these works are quite recent. However to the best of authors' knowledge, articles related to static/dynamic behavior of MEE curved beams are apparently absent. Thus, the scope of this research is directed toward offering some contributions in the mechanics of curved MEE beams.

The present article is arranged according to the following scheme: As first step the hypotheses of the constitutive model are

* Corresponding author at: Centro de Investigaciones de Mecánica Teórica y Aplicada, Universidad Tecnológica Nacional FRBB, 11 de Abril 461, B8000LMI Bahía Blanca, Argentina. Tel.: +54 291 4555220; fax: +54 291 4555311.
E-mail address: mpiovan@frbb.utn.edu.ar (M.T. Piovan).

http://dx.doi.org/10.1016/j.mechrescom.2015.05.003
0093-6413/

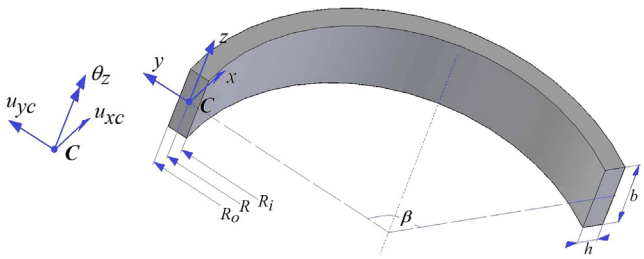

Fig. 1. Sketch of a MEE curved beam.

enunciated and the structural model presented, then an equivalent MEE curved beam model is constructed on the basis of curved beam theories previously developed by authors [15,16]. The structural model is conceived in the context of first order shear theories. An analytical solution is implemented to perform introductory studies. Finally some calculations and parametrical studies are shown in order to characterize some aspects of the dynamics of MEE curved beams. Also a few comparisons of the 1D curved beam model with other approaches and higher order MEE theories (i.e. 1D or/and 2D finite element models) are performed.

2. Deduction of the mechanic model

The MEE structure consists of a thin rectangular strip curved such as the one indicated in Fig. 1, where it is possible to see the circumferential reference system located in the point **C**, i.e. the geometric centroid of the cross section. The curved beam has a circumferential length of $L = R\beta$, a radial thickness of h, width of b and a constant radius of curvature R.

The model of the curved MEE beam is developed by considering the following hypotheses (a) the motion is constrained to the plane XY; (b) the material is assumed to be poled in the radial direction; (c) the electric and magnetic fields are determined through their corresponding potentials which are prescribed at the lateral cylindrical surfaces (i.e. $y = R \pm h/2$, or $y = R_i$, $y = R_o$); (d) the radial components of the electric and magnetic fields are substantially greater than the circumferential components ($E_x \ll E_y$ $H_x \ll H_y$).

Thus, taking into account the aforementioned hypothesis, the following displacement field can be defined [15,17]:

$$\begin{aligned} u_x(x,y,t) &= u_{xc}(x,t) - y\left(\theta_z(x,t) - \frac{u_{xc}(x,t)}{R}\right) \\ u_y(x,y,t) &= u_{yc}(x,t) \end{aligned} \tag{1}$$

where $u_{xc}(x, t)$ and $u_{yc}(x, t)$ are the circumferential and radial displacements of the reference point **C** and $\theta_z(x, t)$ is the rotation parameter. These kinematic variables are described in Fig. 1, and they characterize the motion of a generic cross-section. For the sake of brevity and to contract the notations the symbolism (x, t) is avoided in subsequent deductions. Besides, the representative strain components can be written in terms of the kinematic variables as [15,17]:

$$\begin{aligned} \varepsilon_{xx} &= \left(\frac{\partial u_x}{\partial x} + \frac{u_y}{R}\right)\frac{R}{R+y} = (\varepsilon_{D1} - y\varepsilon_{D2})\mathcal{F} \\ 2\varepsilon_{xy} = \gamma_{xy} &= \left(\frac{\partial u_y}{\partial x} - \frac{u_x}{R}\right)\frac{R}{R+y} + \frac{\partial u_x}{\partial y} = \varepsilon_{D3}\mathcal{F} \end{aligned} \tag{2}$$

where

$$\varepsilon_{D1} = u'_{xc} + \frac{u_{yc}}{R}, \quad \varepsilon_{D2} = \theta'_z - \frac{u'_{xc}}{R}, \quad \varepsilon_{D3} = u'_{yc} - \theta_z, \quad \mathcal{F} = \frac{R}{R+y} \tag{3}$$

In the previous expression and in the subsequent paragraphs, the apostrophes indicate derivatives with respect to the spatial variable x. ε_{D1} can be interpreted as the generalized circumferential strain, ε_{D2} is the generalized bending curvature and ε_{D3} is the generalized shear strain. For the sake of brevity the following definitions of the internal forces are introduced:

$$\{Q_x, Q_y, M_z\} = \int_A \{\sigma_{xx}, \sigma_{xy}, -y\sigma_{xx}\} dA \tag{4}$$

where Q_x is the axial force, Q_y is the shear force and M_z is the bending moment.

The mechanical equilibrium equations of the curved MEE beam can be written in the following form [17]:

$$\begin{aligned} &-Q'_x + \frac{M'_z}{R} + \mathcal{M}_1(\ddot{u}_{xc}, \ddot{u}_{yc}, \ddot{\theta}_z) - \mathcal{P}_1(x) = 0 \\ &-Q'_y + \frac{Q_x}{R} + \mathcal{M}_2(\ddot{u}_{xc}, \ddot{u}_{yc}, \ddot{\theta}_z) - \mathcal{P}_2(x) = 0 \\ &-M'_z - Q_y + \mathcal{M}_3(\ddot{u}_{xc}, \ddot{u}_{yc}, \ddot{\theta}_z) - \mathcal{P}_3(x) = 0 \end{aligned} \tag{5}$$

with the following boundary conditions:

$$\begin{aligned} &-\tilde{Q}_x + \frac{\tilde{M}_z}{R} + Q_x - \frac{M_z}{R} = 0, \quad \text{or} \quad u_{xc} = 0 \\ &-\tilde{Q}_y + Q_y = 0, \quad \text{or} \quad u_{yc} = 0 \\ &-\tilde{M}_z + M_z = 0, \quad \text{or} \quad \theta_z = 0 \end{aligned} \tag{6}$$

In the previous expressions, dots over the kinematic variables identify derivation with respect to the time; $\mathcal{P}_i$, $i = 1, 2, 3$ represent distributed forces and moments, $\tilde{Q}_x$, $\tilde{Q}_y$ and $\tilde{Q}_x$ represent prescribed forces applied at the ends, whereas $\mathcal{M}_i$, $i = 1, 2, 3$ are inertia forces which are defined as:

$$\begin{Bmatrix} \mathcal{M}_1 \\ \mathcal{M}_2 \\ \mathcal{M}_3 \end{Bmatrix} = \begin{bmatrix} J^\rho_{11} & 0 & J^\rho_{13} \\ 0 & J^\rho_{22} & 0 \\ J^\rho_{13} & 0 & J^\rho_{33} \end{bmatrix} \begin{Bmatrix} \ddot{u}_{xc} \\ \ddot{u}_{yc} \\ \ddot{\theta}_z \end{Bmatrix} \tag{7}$$

In Eq. (7) J^ρ_{ik}, $i, k \to 1, 2, 3$ are inertia constants that are described "in-extenso" in Appendix I.

2.1. Deduction of the electric and magnetic potentials

The constitutive equations of a magneto-electro-elastic solid under the hypothesis of plane stress – assuming $\sigma_{yy} \ll \sigma_{xx}$ and employing the hypothesis (d) – can be written in the following matrix form [12,13]:

$$\begin{Bmatrix} \sigma_{xx} \\ \sigma_{xy} \\ D_x \\ D_y \\ B_x \\ B_y \end{Bmatrix} = \begin{bmatrix} c^*_{11} & 0 & -e^*_{21} & -q^*_{21} \\ 0 & c^*_{66} & 0 & 0 \\ 0 & e^*_{16} & 0 & 0 \\ e^*_{21} & 0 & \eta_{22} & d_{22} \\ 0 & q^*_{16} & 0 & 0 \\ q^*_{21} & 0 & d_{22} & \mu_{22} \end{bmatrix} \begin{Bmatrix} \varepsilon_{xx} \\ \gamma_{xy} \\ E_y \\ H_y \end{Bmatrix} \tag{8}$$

and σ_{ij} are the stresses, ϵ_{ij} and γ_{xy} are the axial and shear strain components; D_i and B_i are the components of the electric displacement and the magnetic flux, respectively; E_i and H_i are the components of the electric field and the magnetic field, respectively; c^*_{ik} are elastic coefficients; η_{ij} are the dielectric coefficients; μ_{ij} are the magnetic permeability coefficients; e^*_{ij} are the piezoelectric coefficients; q^*_{ij} are the piezomagnetic coefficients and d_{ij} are the magnetoelectric coefficients.

It is interesting to note that from Eq. (8), the electric displacement and magnetic flux in x-direction (D_x and B_x, respectively) depend only on the shear strain γ_{xy}. These constitutive expressions allow the calculation of the electric and the magnetic potentials in explicit form (see Ref. [12] for detailed issues).

The electric and magnetic fields are defined in terms of the electric and magnetic potentials as:

$$\begin{aligned} \bar{E} &= -\bar{\nabla}\Phi \\ \bar{H} &= -\bar{\nabla}\Psi \end{aligned} \tag{9}$$

where $\bar{\nabla}$ is the gradient operator in curvilinear coordinates.

The equilibrium equations of electrostatics and magnetostatics are [8,18]:

$$\begin{aligned} \bar{\nabla}\cdot\bar{D} &= 0 \\ \bar{\nabla}\cdot\bar{B} &= 0 \end{aligned} \tag{10}$$

where $\bar{D} = \{D_x, D_y, D_z\}$, $\bar{B} = \{B_x, B_y, B_z\}$, and $\bar{\nabla}\cdot$ is the divergence operator (in curvilinear coordinates).

Now, employing Eq. (8) together with Eq. (10) and after some algebraic handling it is possible to arrive to:

$$\begin{Bmatrix} \dfrac{\mathcal{F}}{R}\dfrac{\partial\Phi}{\partial y} + \dfrac{\partial^2\Phi}{\partial y^2} \\ \dfrac{\mathcal{F}}{R}\dfrac{\partial\Psi}{\partial y} + \dfrac{\partial^2\Psi}{\partial y^2} \end{Bmatrix} = \begin{bmatrix} A_{11} & A_{12} \\ A_{21} & A_{22} \end{bmatrix} \begin{Bmatrix} \mathcal{F}^2\varepsilon'_{D3} \\ \mathcal{F}\varepsilon_{D2} \end{Bmatrix} \tag{11}$$

where

$$\begin{bmatrix} A_{11} & A_{12} \\ A_{21} & A_{22} \end{bmatrix} = \begin{bmatrix} \eta_{22} & d_{22} \\ d_{22} & \mu_{22} \end{bmatrix}^{-1} \begin{bmatrix} e^*_{16} & e^*_{21} \\ q^*_{16} & q^*_{21} \end{bmatrix}. \tag{12}$$

The differential system written in Eq. (11) is easy to integrate in the variable y. Thus, employing the following boundary conditions in Eq. (11):

$$\begin{cases} \Phi(x, -h/2) = \Phi_0 \\ \Phi(x, h/2) = \Phi_1 \end{cases}, \quad \begin{cases} \Psi(x, -h/2) = \Psi_0 \\ \Psi(x, h/2) = \Psi_1 \end{cases}, \tag{13}$$

the electric and magnetic potentials can be written as follows:

$$\begin{aligned} \Phi &= \mathcal{D}_1\Phi_0 + \mathcal{D}_2\Phi_1 + \mathcal{D}_3\varepsilon'_{D3} + \mathcal{D}_4\varepsilon_{D2} \\ \Psi &= \mathcal{B}_1\Psi_0 + \mathcal{B}_2\Psi_1 + \mathcal{B}_3\varepsilon'_{D3} + \mathcal{B}_4\varepsilon_{D2} \end{aligned} \tag{14}$$

where the coefficients $\mathcal{D}_i, \mathcal{B}_i, i = 1, \ldots, 4$ are functions of the variable y (see Appendix II), and by employing these potentials, it is possible to arrive to the components of the electric and magnetic fields as:

$$\begin{aligned} E_x &= -\mathcal{F}\bar{\mathcal{D}}\cdot\frac{\partial\bar{\mathcal{E}}}{\partial x}, \quad E_y = -\frac{\partial\bar{\mathcal{D}}}{\partial y}\cdot\bar{\mathcal{E}} \\ H_x &= -\mathcal{F}\bar{\mathcal{B}}\cdot\frac{\partial\bar{\mathcal{H}}}{\partial x}, \quad H_y = -\frac{\partial\bar{\mathcal{B}}}{\partial y}\cdot\bar{\mathcal{H}} \end{aligned} \tag{15}$$

where the following vectors are defined in order to contract notation:

$$\begin{aligned} &\bar{\mathcal{D}} = \{\mathcal{D}_1, \mathcal{D}_2, \mathcal{D}_3, \mathcal{D}_4\}, \quad \bar{\mathcal{B}} = \{\mathcal{B}_1, \mathcal{B}_2, \mathcal{B}_3, \mathcal{B}_4\} \\ &\bar{\mathcal{E}} = \left\{\Phi_0, \Phi_1, \varepsilon'_{D3}, \varepsilon_{D2}\right\}, \quad \bar{\mathcal{H}} = \left\{\Psi_0, \Psi_1, \varepsilon'_{D3}, \varepsilon_{D2}\right\} \end{aligned} \tag{16}$$

2.2. Constitutive model

According to the definition of the internal forces given in Eq. (4) and employing Eq. (8) it is possible to derive the following expression of the internal forces in terms of strain components and electro/magnetic potentials:

$$\begin{Bmatrix} Q_x \\ Q_y \\ M_z \end{Bmatrix} = \begin{bmatrix} J_{X1} & J_{X2} & 0 & J_{X4} \\ 0 & 0 & J_{Y3} & 0 \\ J_{M1} & J_{M2} & 0 & J_{M4} \end{bmatrix} \begin{Bmatrix} \varepsilon_{D1} \\ \varepsilon_{D2} \\ \varepsilon_{D3} \\ \varepsilon'_{D3} \end{Bmatrix} + \begin{bmatrix} J_{X5} & J_{X6} & J_{X7} & J_{X8} \\ 0 & 0 & 0 & 0 \\ J_{M5} & J_{M6} & J_{M7} & J_{M8} \end{bmatrix} \begin{Bmatrix} \Phi_0 \\ \Phi_1 \\ \Psi_0 \\ \Psi_1 \end{Bmatrix} \tag{17}$$

where J_{Xi}, J_{Mi}, J_{Yi}, $i = 1, \ldots, 8$ are constants that depend on the elastic, electric and magnetic properties (the are defined in Appendix I).

2.3. Differential equations of motion for the MEE curved beam

Substituting Eq. (17) in Eq. (5), the following differential equations are deduced:

$$\begin{aligned} &K_{X1}\varepsilon'_{D1} + K_{X2}\varepsilon'_{D2} + K_{X4}\varepsilon''_{D3} + \sum_{i=5}^{8} K_{Xi}\frac{\partial V_{Ei}}{\partial x} + J^{\rho}_{11}\ddot{u}_{xc} + J^{\rho}_{13}\ddot{\theta}_z - \mathcal{P}_1 = 0 \\ &-J_{Y3}\varepsilon'_{D3} + \frac{J_{X1}}{R}\varepsilon_{D1} + \frac{J_{X2}}{R}\varepsilon_{D2} + \frac{J_{X4}}{R}\varepsilon'_{D3} + \sum_{i=5}^{8}\frac{J_{Xi}}{R}V_{Ei} + J^{\rho}_{11}\ddot{u}_{yc} - \mathcal{P}_2 = 0 \\ &-J_{M1}\varepsilon'_{D1} - J_{M2}\varepsilon'_{D2} - J_{M4}\varepsilon''_{D3} - J_{Y3}\varepsilon_{D3} + \sum_{i=5}^{8} J_{Mi}\frac{\partial V_{Ei}}{\partial x} + J^{\rho}_{13}\ddot{u}_{xc} + J^{\rho}_{33}\ddot{\theta}_z - \mathcal{P}_3 = 0 \end{aligned} \tag{18}$$

where

$$K_{Xi} = \frac{J_{Mi}}{R} - J_{Xi}, \quad i = 1, \ldots, 8 \tag{19}$$

$$V_E = \{0, 0, 0, 0, \Phi_0, \Phi_1, \Psi_0, \Psi_1\} \tag{20}$$

The differential system (18) represents the mechanics of a MEE monomorph curved beam. It is the case of a differential system that couples the elastic and electromagnetic fields. The response of this system for given problems can be tackled by means of many approaches (FEM, analytical, etc.). Due to size limitations, in the following paragraph a simple analytical solution for free vibration problems is performed.

2.4. An analytical approach for free vibrations

It is possible to derive a simple analytical solution for the free vibration problem by considering the following hypotheses: (a) the external potential are annulated (i.e. $\Phi_i = \Psi_i = 0, i = 1, 2$) and only the coupling between elastic and electromagnetic properties are considered [12], (b) no external loads are involved (i.e. $\mathcal{P}_i = 0, i = 1, 2, 3$) and (c) simply supported conditions are adopted at the beam ends ($u_{yc} = 0$, $Q_x = 0$, $M_z = 0$). Under these restrictions the kinematic variables can be represented in terms of harmonic functions (sinusoidal and/or complex exponentials) that fulfill the boundary conditions, as it was done in other similar articles [16,19]. Then after algebraic manipulation it is possible to arrive to the following eigenvalue characteristic expression:

$$|\mathbf{K} - \omega^2\mathbf{M}| = 0 \tag{21}$$

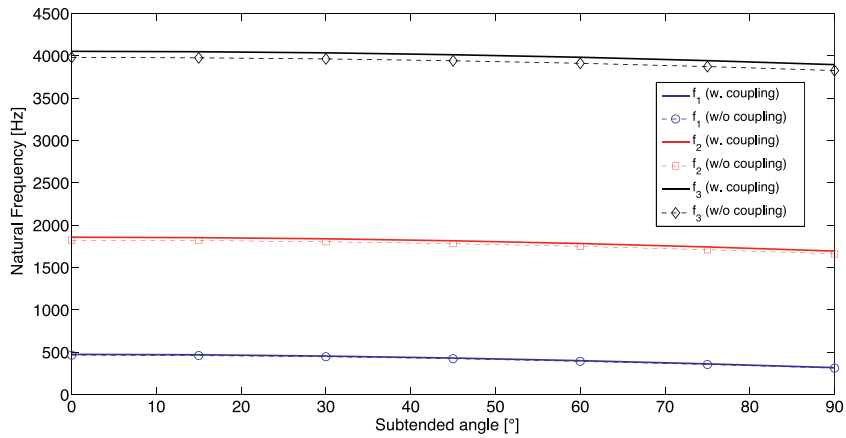

Fig. 2. Variation of the first three natural frequencies [Hz] with respect to the subtended angle.

where

$$\mathbf{K} = \begin{bmatrix} k_i^2\left(\frac{K_{X2}}{R} - K_{X1}\right) & k_i\frac{K_{X1}}{R} - k_i^3 K_{X4} & k_i^2\left(K_{X4} - \frac{K_{X2}}{R}\right) \\ k_i\left(\frac{J_{X2}}{R^2} - \frac{J_{X1}}{R}\right) & \frac{J_{X1}}{R^2} - k_i^2\left(\frac{J_{X4}}{R} - J_{Y3}\right) & k_i\left(\frac{J_{X4} - J_{X2}}{R} - J_{Y3}\right) \\ k_i^2\left(J_{M1} - \frac{J_{M2}}{R}\right) & k_i^3 J_{M4} - k_i\left(\frac{J_{M1}}{R} + J_{Y3}\right) & k_i^2(J_{M2} - J_{M4}) + J_{Y3} \end{bmatrix} \tag{22}$$

$$\mathbf{M} = \begin{bmatrix} J_{11}^{\rho} & 0 & J_{13}^{\rho} \\ 0 & J_{11}^{\rho} & 0 \\ J_{13}^{\rho} & 0 & J_{33}^{\rho} \end{bmatrix} \tag{23}$$

The parameter $k_i = i\pi/L$, $i = 1, 2, 3, \ldots$ is the wave number, $\omega = 2\pi f$ is the circular frequency (rad/s) whereas f is the natural frequency (Hz).

3. Comparisons and examples

In this section some comparisons with available models/approaches and some new results for curved MEE are presented. The material properties of a MEE composite with 40% $BaTiO_3$ and 60% $CoFe_2O_4$ are taken from the works of Biju et al [20] and Annigeri et al. [18] to calculate the beam equivalent electro-elastic coefficients. These coefficients are summarized in Table 1 that, by the way, are quite similar to the ones calculated by Milazzo et al. [12].

The first example corresponds to a comparison of the present curved beam model (reduced to the case of a straight beam) with the results of previous studies about MEE straight beam models [12]. The beam has a length $L = 0.3$ m and a thickness $h = 0.02$ m (a unitary width is considered just for comparison purposes with a 2D plane stress finite element approach). In Table 2 it is possible to see the comparison of the present model (with $R \to \infty$) with previous results (a 1D straight beam approach [12], and a 2D FEM approach [18]). The frequency values are calculated considering zero potentials (i.e. $\Phi_i = \Psi_i = 0$, $i = 1, 2$) and with or without electro-elastic coupling in the material properties (i.e. setting to zero the piezo-electric, $e_{ij}^* = 0$, and piezo-magnetic, $q_{ij}^* = 0$, see Appendix I). As one can see in Table 2 there is a good agreement between the present model reduced to the straight beam case and previous straight beam approaches for MEE [12,18]. The natural frequencies percentage discrepancy with respect to Milazzo's or Annigeri's results is less than 1% in all cases, and reaching no more than 0.2% in the first four modes.

Table 1
Beam Equivalent properties for MEE material (40% $BaTiO_3$ and 60% $CoFe_2O_4$).

	Property				
	c_{11}^* (GPa)	c_{66}^* (GPa)	e_{21}^* (C/m^2)	e_{16}^* (C/m^2)	q_{21}^* (N/(Am))
Values	120.6	45	6.52	0	32.66

	Property				
	q_{16}^* (N/(Am))	η_{22} (Ns/(CV))	d_{22} (F/m)	μ_{22} (Ns^2/C^2)	ρ (kg/m^3)
Values	180	-8.97×10^{-9}	8.85×10^{-9}	7.54×10^{-3}	5600

Table 2
Comparison of free vibration frequencies (Hz) calculated with the present model (with $R \to \infty$) and previous approaches (1D analytical model [12] and FEM: 2D plane stress [18]).

Frequency order	Present model w/o coupling	Present model with coupling	Milazzo et al. [12]	Annigeri et al. [18]
f_1	465	474	475	474
f_2	1822	1857	1861	1858
f_3	3980	4052	4049	4045
f_4	6808	6925	6900	6896
f_5	10,178	10,342	10,272	10,274
f_6	13,969	14,180	14,039	14,056

The second example corresponds to the evaluation of the curved beam model and the variation of the natural frequencies with respect to some parameters. The basic geometric properties of the curved beam are the same of the previous example and maintained unaltered however the curvature radius is varied from the case of a straight beam (i.e. $R \to \infty$) to the case related to a subtended angle of quarter circumference (i.e. $L/R = 90°$).

In Fig. 2 the variation of the first three frequencies of the MEE curved beam with respect to the subtended angle is shown. It is clear that $R \to \infty$ (i.e. $\beta = L/R = 0$) the frequencies correspond to the case of a straight beam. As the subtended angle increases (or the curvature radius decreases) the values of the frequencies decrease. This variation is more sensitive in the first natural frequency (f_1), that decreases from 475 Hz (at $\beta = L/R = 0$) to 318 Hz (at $\beta = L/R = 90°$). This implies a reduction of 33%. The reduction of the other two frequencies shown in Fig. 2 is of 8% and 4% for f_2 and f_3, respectively.

There is another matter shown in Fig. 2, as well as in Table 2, related to the hypothesis employed to calculate the beam cross-sectional coefficients. In fact when these coefficients are calculated avoiding the piezo-electric and piezo-magnetic coupling (always in absence of electric and magnetic potentials) the frequencies obtained are nearly 1.8% lower than their counterparts calculated

employing the full MEE coupling. This aspect was also mentioned in previous studies for straight MEE beams with 2D approaches [18].

4. Conclusions

In this article a new model for analysis of MEE beam with curved configuration has been introduced. The mathematical model is based in the context of linear elasticity and developed as a technical theory for mono-morph MEE beams. The shear deformation has been taken into account. Some new studies about free vibrations of curved MEE beams have been provided. Also the curved beam model can be reduced to models of straight beams (by setting curvature radius to infinity), and it compares quite well with the results of previous MEE straight beam models as well as 2D finite element approaches.

This class of 1D models, due to their inherent computational low cost, should be useful tools for analyzing stochastic problems associated with uncertainties in the material properties, piezo-electro-magnetic loads, and environmental conditions as well as optimization problems in which MEE slender structures are involved, however this is the matter of future work.

Acknowledgements

The authors recognize the support of Universidad Tecnológica Nacional (under Project No. 2194TC) and CONICET of Argentina and also the support of Universidad de las Fuerzas Armadas (ESPE) and SENESCYT of Ecuador under the Program Prometeo.

Appendix I

The inertia constants J^{ρ}_{ik}, $i, k \to 1, 2, 3$ are calculated in the following compact form:

$$J^{\rho}_{ik} = \int_A \rho \bar{g}^{(a)}_i \bar{g}^{(a)}_k \mathcal{F}^{-1} dA + \int_A \rho \bar{g}^{(b)}_i \bar{g}^{(b)}_k \mathcal{F}^{-1} dA \tag{24}$$

in which $\bar{g}^a$ and $\bar{g}^b$ are defined as:

$$\begin{aligned} \bar{g}^{(a)} &= \{\mathcal{F}^{-1}, 0, -y\} \\ \bar{g}^{(b)} &= \{0, 1, 0\} \end{aligned} \tag{25}$$

The beam equivalent MEE constants are defined calculated as:

$$\begin{aligned} J_{X1} &= \int_A c^*_{11} \mathcal{F} dA, \quad J_{X2} = \int_A \left[-c^*_{11} y \mathcal{F} + e^*_{21} \frac{\partial \mathcal{D}_4}{\partial y} + q^*_{21} \frac{\partial \mathcal{B}_4}{\partial y} \right] dA, \\ J_{X4} &= \int_A \left[e^*_{21} \frac{\partial \mathcal{D}_3}{\partial y} + q^*_{21} \frac{\partial \mathcal{B}_3}{\partial y} \right] dA, \quad J_{Y3} = \int_A c^*_{66} \mathcal{F} dA \end{aligned} \tag{26}$$

$$\begin{aligned} J_{M1} &= -\int_A c^*_{11} y \mathcal{F} dA, \quad J_{M2} = \int_A \left[c^*_{11} y^2 \mathcal{F} - e^*_{21} y \frac{\partial \mathcal{D}_4}{\partial y} - q^*_{21} y \frac{\partial \mathcal{B}_4}{\partial y} \right] dA, \\ J_{M4} &= -\int_A y \left[e^*_{21} \frac{\partial \mathcal{D}_3}{\partial y} + q^*_{21} \frac{\partial \mathcal{B}_3}{\partial y} \right] dA, \end{aligned} \tag{27}$$

$$\begin{aligned} \{J_{X5}, J_{X6}, J_{X7}, J_{X8}\} &= \int_A \{e^*_{21}, e^*_{21}, q^*_{21}, q^*_{21}\} \cdot \frac{\partial}{\partial y} \{\mathcal{D}_1, \mathcal{D}_2, \mathcal{B}_1, \mathcal{B}_2\} dA, \\ \{J_{M5}, J_{M6}, J_{M7}, J_{M8}\} &= -\int_A y \{e^*_{21}, e^*_{21}, q^*_{21}, q^*_{21}\} \cdot \frac{\partial}{\partial y} \{\mathcal{D}_1, \mathcal{D}_2, \mathcal{B}_1, \mathcal{B}_2\} dA \end{aligned} \tag{28}$$

Appendix II

Coefficients $\mathcal{D}_i$, and $\mathcal{B}_i$, $i = 1, \ldots, 4$ are calculated in the subsequent Taylor's expansion form:

$$\begin{aligned} \mathcal{D}_1 = \mathcal{B}_1 &= \left(\frac{1}{2} - \frac{y}{h} \right) + \frac{(-h/8) + (y^2/2h)}{R} + \frac{(hy/12) - (y^3/3h)}{R^2} \\ \mathcal{D}_2 = \mathcal{B}_2 &= \left(\frac{1}{2} + \frac{y}{h} \right) + \frac{(h/8) - (y^2/2h)}{R} + \frac{(-hy/12) + (y^3/3h)}{R^2} \end{aligned} \tag{29}$$

$$\begin{aligned} \mathcal{D}_3 &= A_{11} \left[\left(-\frac{1}{8} h^2 + \frac{y^2}{2} \right) + \frac{h^2 y - 4y^3}{8R} + \frac{-5h^4 - 24h^2 y^2 + 176y^4}{384R^2} \right] \\ \mathcal{D}_4 &= A_{12} \left[\frac{1}{8}(h^2 - 4y^2) + \frac{-(1/12)h^2 y + (y^3/3)}{R} + \frac{h^4 + 8h^2 y^2 - 48y^4}{192R^2} \right] \end{aligned} \tag{30}$$

$$\begin{aligned} \mathcal{B}_3 &= A_{21} \left[\left(-\frac{1}{8} h^2 + \frac{y^2}{2} \right) + \frac{h^2 y - 4y^3}{8R} + \frac{-5h^4 - 24h^2 y^2 + 176y^4}{384R^2} \right] \\ \mathcal{B}_4 &= A_{22} \left[\frac{1}{8}(h^2 - 4y^2) + \frac{-(1/12)h^2 y + (y^3/3)}{R} + \frac{h^4 + 8h^2 y^2 - 48y^4}{192R^2} \right] \end{aligned} \tag{31}$$

References

[1] D. Saravanos, P. Heyliger, Mechanics and computational models for laminated piezoelectric beams, plates and shells, Appl. Mech. Rev. 52 (1999) 305–320.
[2] C. Nan, Magnetoelectric effect in composites of piezoelectric and piezomagnetic phases, Phys. Rev. B 50 (1994) 6082–6088.
[3] T. Bui, M. Nguyen, C. Zhang, K. Pham, An efficient meshfree method for analysis of two-dimensional piezoelectric structures, Smart Mater. Struct. 20 (2011) 016–065.
[4] P. Heyliger, Exact solutions for simply supported laminated piezoelectric plates, J. Appl. Mech. 64 (1997) 299–306.
[5] P. Heyliger, F. Ramirez, E. Pan, Two dimensional static fields in magnetoelectroelastic laminates, J. Intell. Mater. Syst. Struct. 15 (9) (2004).
[6] E. Pan, Exact solution for simply supported and multilayered magneto-electro-elastic plates, J. Appl. Mech. 68 (2001) 608–618.
[7] E. Pan, P. Heyliger, Exact solutions for magneto-electro-elastic laminates in cylindrical bending, Int. J. Solids Struct. 40 (2003) 6859–6876.
[8] J. Chen, H. Chen, E. Pan, P. Heyliger, Modal analysis of magneto-electro-elastic plates using the state-vector approach, J. Sound Vib. 304 (2007) 722–734.
[9] E. Pan, P. Heyliger, Free vibration of simply supported and multilayered magneto-electro-elastic plates, J. Sound Vib. 252 (2002) 429–442.
[10] C.-P. Wu, Y.-C. Lu, A modified Pagano method for the 3d dynamic responses of functionally graded magneto-electro-elastic plates, Compos. Struct. 90 (2009) 363–372.
[11] Y.-H. Tsai, C.-P. Wu, Y.-S. Syu, Three-dimensional analysis of doubly curved functionally graded magneto-electro-elastic shells, Eur. J. Mech. A: Solids 27 (2008) 79–105.
[12] A. Milazzo, C. Orlando, A. Alaimo, On the shear influence on the free vibration behavior of magneto-electro-elastic beam, in: International Conference on Computational and Experimental Engineering and Sciences, vol. 11 (No. 2), 2009, pp. 55–61.
[13] A. Milazzo, C. Orlando, A beam finite element for magneto-electro-elastic multilayered composite structures, Compos. Struct. 94 (12) (2012) 3710–3721.
[14] A. Milazzo, A one dimensional model for dynamic analysis of generally layered magneto-electro-elastic beams, J. Sound Vib. 332 (2) (2013) 465–483.
[15] M. Piovan, V. Cortínez, Mechanics of thin-walled curved beams made of composite materials, allowing for shear deformability, Thin-Walled Struct. 45 (2007) 759–789.
[16] C. Filipich, M. Piovan, The dynamics of thick curved beams constructed with functionally graded materials, Mech. Res. Commun. 37 (2010) 565–570.
[17] M. Piovan, C. Filipich, J. Ramirez, A model for shear deformable curved beam made of functionally graded materials, Mec. Comput. 27 (2008) 2053–2067.
[18] A. Annigeri, N. Ganesan, S. Swarnamani, Free vibration behaviour of multiphase and layered magneto-electro-elastic beam, J. Sound Vib. 299 (2007) 44–63.
[19] M. Piovan, S. Domini, J. Ramirez, In-plane and out-of-plane dynamics and buckling of functionally graded circular curved beams, Compos. Struct. 9 (2012) 3194–3206.
[20] B. Biju, N. Ganesan, K. Shankar, Response of multiphase magneto-electro-elastic sensors under harmonic mechanical loading, Int. J. Eng. Sci. Technol. 1 (1) (2009) 216–227.